OPEN ACCESS

Original research

Placental mesenchymal stem cells boost M2 alveolar over M1 bone marrow macrophages via IL-1β in *Klebsiella*-mediated acute respiratory distress syndrome

Li-Tzu Wang,[1] B Linju Yen,[2,3] Hsiu-Huan Wang,[2] Ying-Yin Chao,[2] Wei Lee,[2,4] Li-Yueh Huang,[5] Sheng-Kang Chiu,[6,7] L. Kristopher Siu,[5,6,8] Ko-Jiunn Liu,[9,10,11,12] Huey-Kang Sytwu,[5,13] Men-Luh Yen[1]

► Additional supplemental material is published online only. To view, please visit the journal online (http://dx.doi.org/10.1136/thoraxjnl-2021-217928).

For numbered affiliations see end of article.

Correspondence to
Professor Men-Luh Yen, Department of Obstetrics & Gynecology, National Taiwan University College of Medicine, Taipei, Taiwan; mlyen@ntu.edu.tw and Professor B Linju Yen, Regenerative Medicine Research Group, Institute of Cellular & System Medicine, National Health Research Institutes, Zhunan, Taiwan; blyen@nhri.edu.tw

BLY and M-LY contributed equally.

Received 9 July 2021
Accepted 30 March 2022
Published Online First 21 April 2022

Check for updates

© Author(s) (or their employer(s)) 2023. Re-use permitted under CC BY. Published by BMJ.

To cite: Wang L-T, Yen BL, Wang H-H, *et al*. *Thorax* 2023;**78**:504–514.

ABSTRACT

Rationale Acute respiratory distress syndrome (ARDS) is a lethal complication of severe bacterial pneumonia due to the inability to dampen overexuberant immune responses without compromising pathogen clearance. Both of these processes involve tissue-resident and bone marrow (BM)–recruited macrophage (MΦ) populations which can be polarised to have divergent functions. Surprisingly, despite the known immunomodulatory properties of mesenchymal stem cells (MSCs), simultaneous interactions with tissue-resident and recruited BMMΦ populations are largely unexplored.

Objectives We assessed the therapeutic use of human placental MSCs (PMSCs) in severe bacterial pneumonia with elucidation of the roles of resident alveolar MΦs (AMΦs) and BMMΦs.

Methods We developed a lethal, murine pneumonia model using intratracheal infection of a clinically relevant *Klebsiella pneumoniae* (KP) strain with subsequent intravenous human PMSC treatment. Pulmonary AMΦ and recruited BMMΦ analyses, histological evaluation, bacterial clearance and mice survival were assessed. To elucidate the role of resident AMΦs in improving outcome, we performed AMΦ depletion in the KP-pneumonia model with intratracheal clodronate pretreatment.

Measurements and main results Human PMSC treatment decreased tissue injury and improved survival of severe KP-pneumonia mice by decreasing the presence and function of recruited M1 BMMΦ while preserving M2 AMΦs and enhancing their antibacterial functions. Interestingly, PMSC therapy failed to rescue AMΦ-depleted mice with KP pneumonia, and PMSC-secreted IL-1β was identified as critical in increasing AMΦ antibacterial activities to significantly improve pathogen clearance—especially bacteraemia—and survival.

Conclusions Human PMSC treatment preferentially rescued resident M2 AMΦs over recruited M1 BMMΦs with overall M2 polarisation to improve KP-related ARDS survival.

Key messages

What is already known on this topic

⇒ Severe bacterial pneumonia often results in acute respiratory distress syndrome (ARDS), a lethal complication due to overexuberant immune responses which cause tissue injury without effective pathogen clearance.

⇒ These processes involve tissue-resident alveolar macrophages (AMΦ) as well as recruited bone marrow (BM) MΦs, both of which can be further polarised to have divergent functions.

⇒ However, no previous reports have studied human mesenchymal stem cell (MSC) interactions with these two different MΦ populations simultaneously in a clinically relevant model.

What this study adds

⇒ We studied the possible therapeutic role of human placental MSCs (PMSCs) in a murine severe bacterial pneumonia/ARDS model using a clinically derived *Klebsiella pneumonia (*KP) strain, and found that human PMSC treatment preferentially rescued resident M2 AMΦs over recruited M1 BMMΦs with overall M2 polarisation of all MΦs to improve severe KP pneumonia/ARDS survival.

How this study might affect research, practice and/or policy

⇒ Our findings demonstrate the distinct roles of different sources of MΦ populations and their polarisation in bacterial infection and recovery, as well as strongly implicate a potential therapeutic role for PMSCs in severe bacterial pneumonia/ARDS.

INTRODUCTION

Acute respiratory distress syndrome (ARDS) is still a lethal complication of severe bacterial pneumonia, with *Klebsiella pneumoniae* (KP) among the most common causative agents.[1] A Gram-negative bacterium with high multidrug resistance and over 80 serotypes, drug design and vaccine development has been difficult for KP.[2 3] Among virulent KP members, the K2 serotype is the most studied since it can cause highly lethal bacterial pneumonia clinically.[4] While previous reports demonstrated that augmenting the innate immune response is

Thorax: first published as 10.1136/thoraxjnl-2021-217928 on 21 April 2022. Downloaded from http://thorax.bmj.com/ on March 20, 2024 by guest. Protected by copyright.

effective,[5 6] both bacteraemia and overexuberant inflammation damaged multiple organs/tissues.[7] Blockage of acute infection mediators including tumour necrosis factor (TNF)-α muted organ/tissue damage but did not improve survival,[8] showing that careful balancing of the bactericidal immune response against excessive inflammation is critical for disease resolution. Recent clinical trials using corticosteroids—arguably the most potent anti-inflammatory agent—to mitigate excessive host responses have not consistently reduced mortality,[9] necessitating better strategies to combat severe bacterial pneumonia or acute respiratory distress syndrome (ARDS).

Multilineage mesenchymal stem cells (MSCs) have been isolated from diverse post-natal sources including the placenta, a temporary organ with fetal contributions which is ethically compliant and easily accessible.[10] MSC sources including placental MSCs (PMSCs) not only have regenerative properties but also strong immunomodulation with therapeutic value.[11–13] Surprisingly, despite well-established interactions of MSCs with adaptive and innate immune cells like T lymphocytes and natural killer cells, respectively,[14] reports on MSC-macrophage (MΦ) interactions are relatively scarce. Moreover, there are almost no MSC studies in which different populations of MΦs are simultaneously evaluated, despite the clear understanding currently that tissue-resident MΦs—important in maintaining tissue/organ homeostasis—are functionally and developmentally distinct from bone marrow (BM)–derived MΦs,[15] which are among the most potent effector cells in host responses against pathogens. The lungs, being in constant interactions with environmental pathogens and toxins, has a resident MΦ population to maintain homeostasis: the alveolar MΦ (AMΦ), derived from the yolk sac.[16 17] When local infection occurs, AMΦs are the first in line to mount an immune response and recruit effector BMMΦs for effective elimination of respiratory pathogens.[15] Both pathogen clearance and tissue damage in bacterial ARDS have been linked to MΦ activity, but the existence of two populations of MΦs during pulmonary infection—resident AMΦs and recruited BMMΦs—makes it difficult to resolve which population is responsible for tissue injury versus disease resolution. Furthermore, all MΦs can undergo functional polarisation into classically activated or M1 MΦs, crucial in fighting off invading pathogens, or alternatively activated or M2 MΦs which are important in tissue repair.[18 19] An imbalance in MΦ polarisation can influence disease outcome, ranging from successful resolution to persistent infection with tissue injury.[17] Given the strong immunomodulatory properties of MSCs and the protean impact of MΦ populations in health and disease, we studied the possible therapeutic role of MSCs for severe bacterial pneumonia/ARDS in a murine disease model and the mechanisms involved using a clinically relevant and virulent KP strain.

METHODS

A detailed description of the methods is provided in the online supplemental information.

Cell culture

Human PMSCs were isolated from term placental tissue obtained after institutional board approval as previously reported, and cultured as previously reported.[10 20]

Mouse model of KP-induced bacterial pneumonia and PMSC injection

A clinical KP strain of serotype 2 was isolated from patient sputum[1] for intratracheally inoculation into C57BL/6 mice at a sublethal or lethal dose (5×10^6 or 5×10^7 CFUs, respectively) according to previous report.[5] PMSCs (3×10^5 cells) or phosphate buffered saline (PBS) were intravenously injected 2 hours after KP injection. Mice were euthanised with CO_2 at 4 hours, with peripheral blood collected for evaluation of bacterial load and lungs collected for evaluation of bacterial load, MΦ analyses and histological evaluation.

Assessment of in vivo MΦ function

Single-cell suspensions derived from lung lobes were stained with antibodies recognising CD45, CD11b, F4/80, CD206, inducible nitric oxide synthase (iNOS), arginase-1 (Arg1), TNF-α (all from eBioscience, San Diego, California, USA), or 2′,7′-dichlorofluorescein diacetate (DCFDA, Sigma-Aldrich, Missouri, USA) for 30 min according to manufacturer's instructions, then assessed by flow cytometry or analysed with t-distributed stochastic neighbor embedding (t-SNE)-based algorithm.[20 21]

In vivo depletion of AMΦs

C57BL/6J mice were intratracheally injected with 100 μL of PBS or 15 mM clodronate (Cayman Chemical, Ann Arbor, Michigan, USA).[22] After 48 hours, the frequency and absolute numbers of $CD11b^{low}F4/80^{+}$ AMΦs and $CD11b^{high}F4/80^{+}$ BMMΦs in lung tissues were assessed by flow cytometry.

Statistics

For comparisons between two groups, non-parametric Mann-Whitney test was used, while for comparisons between multiple groups, non-parametric analysis of variance was used followed by Dunn's test. Comparisons of survival curves were made using Kaplan-Meier method with *log*-rank tests. A value of $p<0.05$ was considered statistically significant. Analyses were performed using GraphPad Prism software (California, USA), and data are shown as mean±SD.

RESULTS

Pulmonary KP infection dramatically decreases resident AMΦs while increasing recruited BMMΦs in the lungs

To assess whether MΦs are critically involved during K2 KP pneumonia, we first performed bioinformatics analysis which demonstrated broad transcriptomic changes in lung tissue from control versus KP-infected mice (figure 1A), and found MΦ-related pathways to be highly enriched (figure 1B). To further delineate immune responses at the cellular level, we performed analyses on immune cells at 2 (h2) and 4 hours (h4) in lungs infected with an LD_{50} of a clinically isolated serotype K2 KP, revealing a dramatic shift in the pattern of lung-isolated MΦs at h2 versus h4 post-infection in comparison to control/PBS-injected mice by t-SNE (figure 1C), with significant increases at h4 post-infection in a population designated G1 which is identified as $CD11b^{high}$MΦs (figure 1D–F). A population designated G2 and identified as $CD11b^{low}$ MΦs was significantly decreased at h4 post-infection (figure 1E,F). These MΦ populations can be further differentiated on $CD11b^{high}$ (G1) and $CD11b^{low}$ (G2) expression as BMMΦs and AMΦs, respectively.[16] Flow cytometric analyses confirmed these findings, showing an increase in the frequency as well as absolute number of BMMΦs over AMΦs at h4 (figure 1G–I). These results demonstrate that K2 KP infection rapidly decreased resident AMΦs while gradually increasing recruited BMMΦs to cause an imbalance in pulmonary MΦ populations, which possibly contribute to subsequent ARDS.

Thorax: first published as 10.1136/thoraxjnl-2021-217928 on 21 April 2022. Downloaded from http://thorax.bmj.com/ on March 20, 2024 by guest. Protected by copyright.

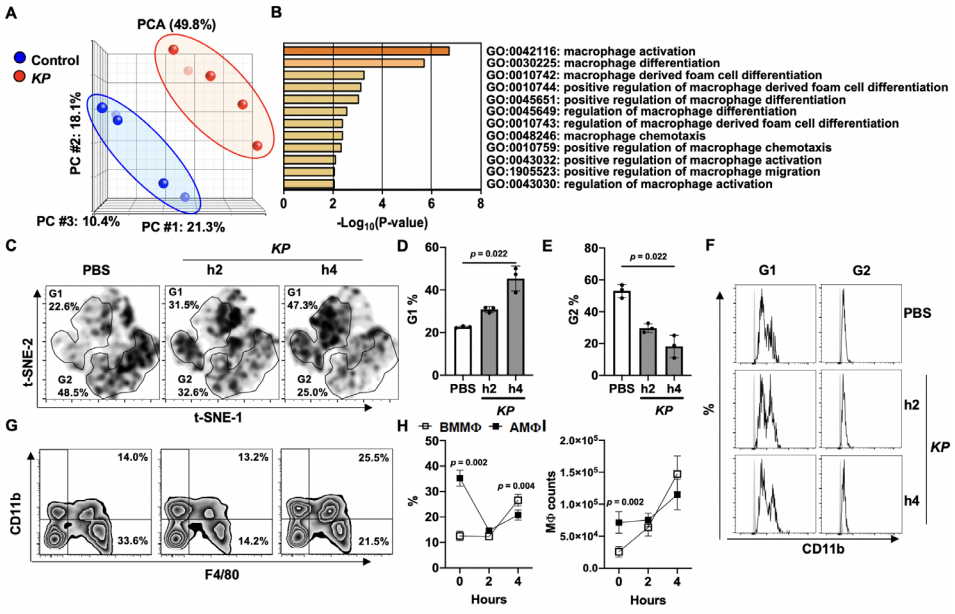

Figure 1 Pulmonary infection of a clinically isolated *Klebsiella pneumonia* (KP)-serotype K2 dramatically decreases resident alveolar macrophages (AMΦs) while increasing recruited bone marrow (BM) MΦs in the lungs. (A) Principal component analysis (PCA) of transcriptomic profiles (National Center for Biotechnology Information-Gene Expression Omnibus or NCBI-GEO database: GSE121970) of KP-infected (n=5) compared to uninfected (n=5) murine lung tissues. The first principal component (PC1) accounts for the largest data variance at 21.3%, while data variance was 18.1% for PC2, and 10.4% for PC3. (B) Metascape pathway analysis for MΦ-related pathways using transcriptomic data of KP-infected murine lung tissue compared with uninfected control, with pathways coloured according to p values. (C) Representative data of t-distributed stochastic neighbor embedding (t-SNE) plots for analyses of changes in MΦs harvested from lung tissues of C57BL/6J mice after intratracheal injection of phosphate buffered saline (PBS; no infection), or infection with sublethal dose (5×10^6 CFUs) of K2 KP for 2 or 4 hours (h2 or h4). Single-cell suspensions derived from lung lobes were stained with anti-CD45, anti-CD11b and anti-F4/80 for flow cytometric analysis, with gating on $CD45^+F4/80^+$ cells for analysis of MΦ populations using tSNE-based algorithm. G1 and G2 were then manually gated on the t-SNE plot by signal profiles. (D, E) Pooled data for G1 and G2 as defined in (C) (n=3 for each group). (F) Histogram graph for CD11b expression levels in G1 representing $CD11b^{high}$ MΦs or and G2 representing $CD11b^{low}$ MΦs as defined in (C). (G) Representative data for frequency analysis of recruited BMMΦs and resident AMΦs in lung lobes taken from uninfected (PBS) and sublethally KP-infected mice sacrificed at h2 and h4 as assessed by flow cytometry. Immune cells harvested from lung tissues were stained with anti-CD45, anti-CD11b and anti-F4/80. Gating for $CD45^+$ cells was first performed, with subsequent frequency analysis for $CD11b^{high}F4/80^+$ and $CD11b^{low}F4/80^+$ to identify for BMMΦs and AMΦs, respectively. (H, I) Pooled data for frequency and absolute numbers, respectively, of BMMΦs (□) and AMΦs (■) in lung lobes as assessed by flow cytometry, with gating for $CD45^+$ cells first and then analysis for cell numbers of $CD11b^{high}F4/80^+$ and $CD11b^{low}F4/80^+$ identified as BMMΦs and AMΦs, respectively (n=6 for each group). Data are shown as mean±SD.

Human PMSCs reduce recruitment of BMMΦs while preserving AMΦs in KP-infected lungs

To elucidate the mechanism underlying the interaction of recruited BMMΦs and resident AMΦs in KP pneumonia, we first used the Molecular Activation Prediction (MAP) tool from Ingenuity Pathway Analysis (IPA) which revealed that during pulmonary KP infection, for the process of BMMΦ migration, many inflammatory cytokines including CXCL3, CCL2 and TNF-α were involved, while for the process of AMΦ quantity, other cytokines including CSF1, CXCL17 and interleukin (IL)-36γ were highly activated (figure 2A). Among these predicted cytokines, TNF-α has been reported as critical in causing pneumonia exacerbation by several infectious agents including KP.[23–25] We therefore performed transcriptomic analyses in TNF-α-treated BMMΦs and found that multiple inflammatory pathways involving either innate or adaptive immunity were activated (figure 2B). To validate the strong presence of TNF-α during in vivo KP pneumonia and assess whether PMSC therapy could limit the highly inflammatory process represented by this cytokine, we detected TNF-α secretion in harvested lung immune cells from uninfected or KP-infected mice 2 hours post-infection which were then co-cultured ex vivo with PMSCs for another 2 hours (figure 2C). We found that PMSCs significantly decreased levels of KP-induced TNF-α even at this early time point post-infection; interestingly, this early post-infection time point is prior to recruited BMMΦs arriving in the lungs (figure 1H,I). We then further assessed PMSC interactions with both AMΦ and BMMΦ populations (figure 2D), and found both percentages (figure 2E) and absolute counts (figure 2F) of BMMΦs were significantly increased whether treated with PBS or PMSCs after KP infection, while a slight but non-significant decrease in absolute BMMΦ numbers after PMSC treatment compared with after PBS treatment in infected mice was seen. Moreover, while BMMΦ expression of CD11b—a critical adhesion molecule involved in recruited BMMΦ tissue migration[26]—was significantly increased after KP infection, PMSC but not PBS treatment resulted in a significant decrease back to nearly baseline levels (figure 2G,H). Furthermore, after KP infection, AMΦ percentages (figure 2I) were significantly decreased when only PBS was given; PMSC treatment, on the other hand, significantly rescued percentages figure 2J. The supportive effects of PMSCs on AMΦs during KP infection were also seen when absolute cell counts were assessed (figure 2J), in which PMSC treatment nearly doubled the average number of AMΦs compared with PBS treatment. Responses of BMMΦ and AMΦ absolute numbers were further confirmed in $CD11c^-SIGLEC\text{-}F^-$ and $CD11c^+SIGLEC\text{-}F^+$ cells

Thorax: first published as 10.1136/thoraxjnl-2021-217928 on 21 April 2022. Downloaded from http://thorax.bmj.com/ on March 20, 2024 by guest. Protected by copyright.

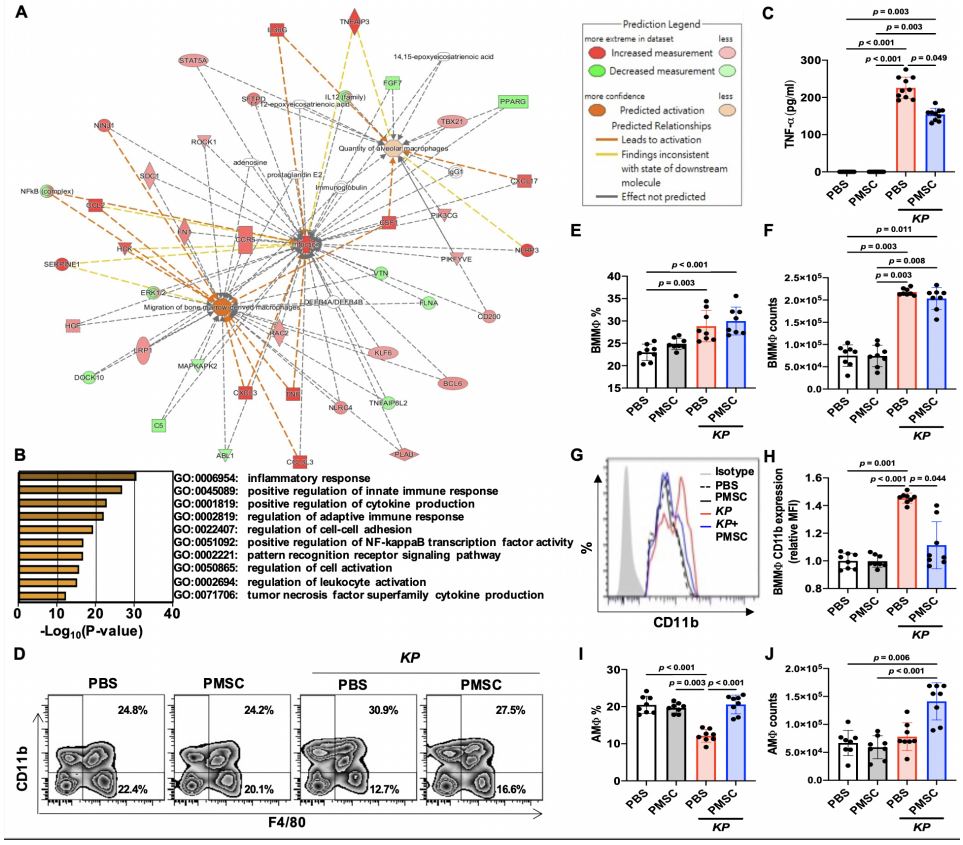

Figure 2 Human placenta mesenchymal stem cells (PMSCs) prevent bone marrow MΦ (BMMΦ) recruitment but preserve alveolar MΦ (AMΦ) population in *Klebsiella pneumoniae* (KP)-infected lungs. (A) Pathway analyses of transcriptomic profiles obtained from KP-infected versus uninfected lung lobes (NCBI-GEO database: GSE121970) as performed with Molecular Activation Prediction (MAP) tool in Ingenuity Pathway Analysis (IPA), for prediction of mechanisms involved in migration of recruited BMMΦs or quantity of resident AMΦs during pulmonary KP infection. IPA showed regulatory relationships between downregulated (green) and upregulated (red) proteins; the MAP tool showed that 'migration of BMMΦs' and 'quantity of AMΦs' are upregulated (orange) through positively regulated downstream molecules (orange lines) or inconsistent findings on some mediators (yellow lines) after occurrence of KP pneumonia (red). (B) Enrichment of immune-related pathways as assessed in transcriptomic data of tumour necrosis factor (TNF)-α-treated BMMΦs versus control BMMΦs (NCBI-GEO database: GSE160163) using Metascape analysis and coloured by p values. (C) Assessment of ex vivo lung inflammation with detection of TNF-α in non-infected and KP-infected lung tissues after phosphate buffered saline (PBS) and PMSC treatment. Mice were intratracheally infected with 5×10^6 CFUs of K2 KP for 2 hours, and then sacrificed for extraction of lung immune cells which were ex vivo co-cultured with human PMSCs at the ratio of 10:1 for 2 hours further and supernatants collected for TNF-α detection (n=10 for each group). (D) Representative data for frequency analysis of recruited BMMΦs and resident AMΦs in lung lobes as assessed with flow cytometry. C57BL/6J mice were intratracheally injected with 5×10^6 CFUs of K2 KP followed by intravenous administration of PBS or 3×10^5 PMSCs 2 hours later. Single-cell suspensions harvested from lung tissues of non-infected mice as well as infected mice injected with PBS or PMSCs were stained with anti-CD45, anti-CD11b and anti-F4/80 for flow cytometric analysis. Gating for $CD45^+$ cells was first performed, with subsequent frequency analysis for $CD11b^{high}F4/80^+$ BMMΦs and $CD11b^{low}F4/80^+$ AMΦs. (E, F) Pooled data for analyses of frequency and absolute counts of recruited BMMΦs in lung lobes of each experimental group, respectively (n=8 for each group). (G, representative data; H, pooled data) Relative CD11b expression levels of recruited BMMΦs in lung lobes of each experimental group by flow cytometric analysis (n=8 for each group). (I, J) Pooled data for analyses of frequency and absolute number of resident AMΦs in lung lobes of each experimental group, respectively (n=8 for each group). Data are shown as mean±SD.

of $CD11b^{high}F4/80^+$ and $CD11b^{low}F4/80^+$ MΦs, respectively (online supplemental figure 1). These results suggest that PMSC administration can prevent recruitment and function of BMMΦs—likely through downregulation of KP-induced TNF-α—while significantly preserving resident AMΦs.

Human PMSCs decrease pulmonary inflammation and tissue injury, as well as significantly increase survival of mice with KP pneumonia

To determine PMSC therapeutic effects on bacterial clearance and tissue injury in KP pneumonia, we first assessed bacterial load and found that PMSC treatment significantly reduced bacterial numbers in infected lungs and decreased incidence of bacteraemia in LD_{50}-infected mice at 4 hours (figure 3A,B). PMSCs also significantly downregulated levels of *KP*-induced TNF-α within lung tissues (online supplemental figure 2), suggesting TNF-α-mediated immunity was not critical for bacterial clearance after PMSC administrated. We then assessed lung tissues of uninfected and infected mice 4 hours after LD_{50} infection histologically (figure 3C). H&E staining of lung tissue sections showed that KP infection increased immune cell infiltration (figure 3C-c), oedematous changes (figure 3C-g) and bronchial epithelium hyperplasia (figure 3C-k), which collectively indicated significant tissue injury similar to ARDS (figure 3D). These changes were reduced (figure 3C-d,h,l) after PMSC treatment. To confirm the degree of inflammatory infiltrates, we also

Thorax: first published as 10.1136/thoraxjnl-2021-217928 on 21 April 2022. Downloaded from http://thorax.bmj.com/ on March 20, 2024 by guest. Protected by copyright.

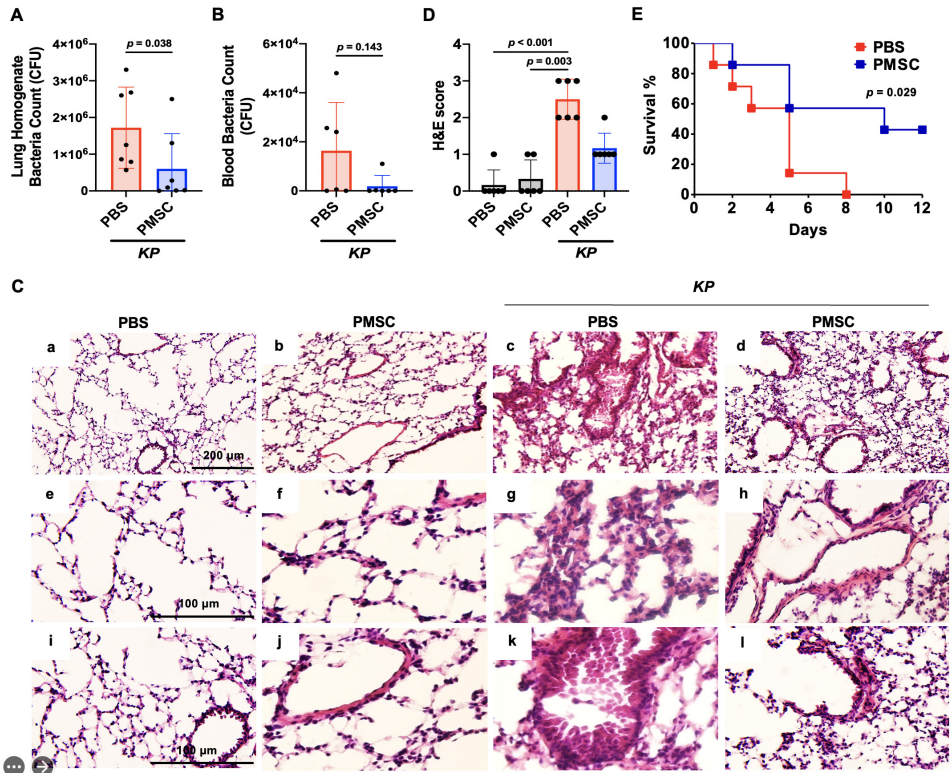

Figure 3 Human placental mesenchymal stem cells (PMSCs) decrease pulmonary inflammation and tissue injury, as well as significantly increase survival of mice with *Klebsiella pneumoniae* (KP) pneumonia. (A, B) Assessment of bacterial load within lung homogenate (A; n=7 for each group) and peripheral blood (B; n=6 for each group). Mice were intratracheally injected with a 5×10^6 CFUs of K2 KP followed by intravenous administration of phosphate buffered saline (PBS) or 3×10^5 PMSCs 2 hours later, with lung lobes excised and peripheral blood collected for CFU calculation. (C, representative data; D, pooled data) H&E staining of histological sections of lung tissues from KP-infected mice after PBS or PMSC treatment (n=6 for each group). Upper panel (a–d): scale bar, 200 µm. Middle (e–h) and bottom panels (i–l), magnifications of lung parenchyma and airways, respectively: scale bar, 100 µm. (E) Kaplan-Meier survival analysis of infected mice treated with or without PMSC treatment. Wild-type C57BL/6J mice were intratracheally injected with a lethal dose (5×10^7 CFUs) of K2 KP followed by intravenous administration of PBS or 3×10^5 PMSCs 2 hours later. Survival was observed for 12 days (n=7 for each group). Data are shown as mean±SD.

collected whole lungs of non-infected and infected mice after PBS or PMSC treatment for analysis of white blood cell (WBC) frequency and cell numbers at 4 hours post-infection. Pulmonary WBC frequency was relatively unchanged 4 hours post-infection (online supplemental figure 3A,B), but absolute numbers were significantly increased, which after PMSC administration was partially reversed (online supplemental figure 3C). To assess whether PMSCs are therapeutic for KP-induced pneumonia/ARDS, intravenously PBS or PMSCs was injected 2 hours after LD_{100} KP infection, and we found that PMSC administration significantly improved KP-infected mice survival rates from 0% to 42.86% (figure 3E). Collectively, these findings demonstrate that PMSC intravenous administration decreased bacterial load, local inflammation and lung tissue injury, to result in significantly improved overall survival of mice with K2 KP pneumonia.

Human PMSCs preserve resident AMΦs over BMMΦs and drive the overall milieu to an M2 immunomodulatory phenotype in mice with KP pneumonia

To assess whether PMSCs can affect polarisation of BMMΦs and/or AMΦs, we first analysed the functional M1 and M2 polarisation markers iNOS and Arg1, respectively. After *KP* infection, iNOS expression (figure 4A,B) was significantly increased but Arg1 expression (figure 4C,D) was significantly decreased in BMMΦs with PBS treatment when compared with uninfected groups; interestingly, expression of both markers was significantly reversed with PMSC treatment. For AMΦs, iNOS expression levels were similar in both uninfected and infected mice (figure 4E,F); however, Arg1 expression was slightly decreased in infected mice with PBS treatment when compared with uninfected groups although non-significantly, but could be significantly reversed with PMSC treatment (figure 4G,H).

To further delineate whether PMSCs can modulate the polarisation of both BMMΦs and AMΦs simultaneously, we first performed t-SNE analyses to visualise the complex changes. Concatenation of all experimental groups demonstrated that the majority of recruited BMMΦs are of the M1 phenotype (identified as $CD206^{low}$), whereas the majority of resident AMΦs are of the M2 phenotype (identified as $CD206^{high}$) (figure 5A). Visualisation of individual experimental groups shows that after KP infection, M1 BMMΦs were more prominent, whereas M2 AMΦs were less prominent, with PMSC treatment after KP infection rescuing M2 AMΦ presence (figure 5B). Confirmation with flow cytometric analyses (figure 5C, representative data) demonstrated that both percentages (figure 5D) and counts (figure 5E) of M1 BMMΦs treated with PBS were significantly increased from uninfected levels which were reversed by PMSC treatment. However, when compared with uninfected groups, M2 BMMΦs percentages (figure 5F) were significantly decreased to similar levels in KP-infected mice whether treated with PBS or

Thorax: first published as 10.1136/thoraxjnl-2021-217928 on 21 April 2022. Downloaded from http://thorax.bmj.com/ on March 20, 2024 by guest. Protected by copyright.

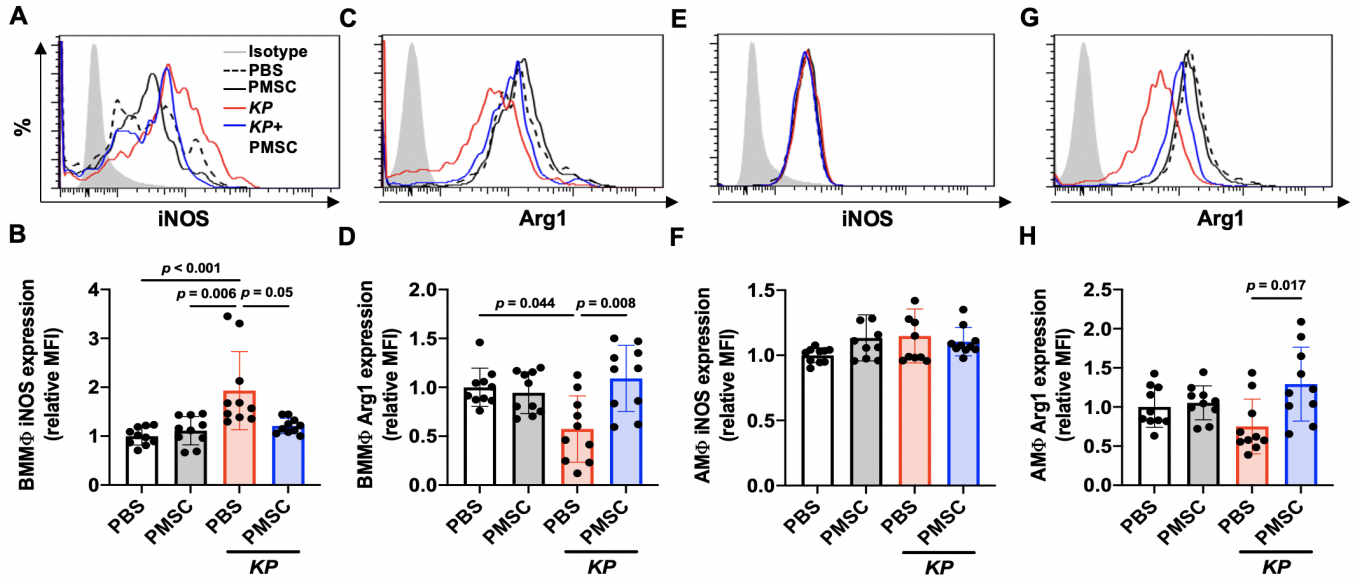

Figure 4 Human PMSCs modulate both bone marrow MΦs (BMMΦs) and alveolar MΦs (AMΦs) to M2 polarisation in mice with *Klebsiella pneumoniae* (KP) pneumonia. (A, representative data; B, pooled data) Relative inducible nitric oxide synthetase (iNOS) expression levels of CD11b^{high}F4/80^{+} BMMΦs in lung lobes of each experimental group as assessed by flow cytometry (n=10 for each group). (C, representative data; D, pooled data) Relative arginase-1 (Arg1) expression levels of CD11b^{high}F4/80^{+} BMMΦs in lung lobes of each experimental group as assessed by flow cytometry (n=10 for each group). (E, representative data; F, pooled data) Relative iNOS expression levels of CD11b^{low}F4/80^{+} AMΦs in lung lobes of each experimental group as assessed by flow cytometry (n=10 for each group). (G, representative data; H, pooled data) Relative Arg1 expression levels of CD11b^{low}F4/80^{+} AMΦs in lung lobes of each experimental group as assessed by flow cytometry (n=10 for each group). Data are shown as mean±SD.

PMSCs, while absolute counts (figure 5G) in infected mice were significantly increased only with treatment of PMSCs but not PBS. When we turned to evaluate polarised subpopulations of AMΦs, we found that both percentages (figure 5H) and absolute counts (figure 5I) of M1 AMΦs were significantly increased from uninfected levels whether treated with PBS or PMSCs. However, PBS treatment significantly decreased M2 AMΦs percentages (figure 5J), while absolute counts (figure 5K) were similar to those in uninfected mice; PMSC treatment in infected mice, on the other hand, not only significantly reversed M2 AMΦ percentages as well as increased absolute counts compared with levels in uninfected mice. Since M1 MΦs are also an important source of TNF-α, we next assessed whether PMSCs can modulate TNF-α expression levels in M1 subpopulation of both BMMΦs and AMΦs. We found that in uninfected mice, treatment with PBS or PMSCs did not change TNF-α levels significantly in M1 BMMΦs, while in infected mice, TNF-α levels in M1 BMMΦs was increased with PBS treatment but significantly reversed with PMSC treatment (figure 5L,M). Interestingly, there were no significant changes in TNF-α levels of M1 AMΦs between uninfected and infected mice regardless of PBS or PMSC treatment (figure 5N,O). Collectively, PMSC treatment can modulate both BMMΦs and AMΦs towards a more M2, tolerogenic response in pulmonary KP infection with particular preservation of M2 AMΦs.

Human PMSCs enhance multiple antibacterial functions in AMΦs but not BMMΦs to significantly improve bacterial clearance and survival in mice with KP pneumonia which were abrogated after AMΦ depletion

To investigate how the prominent immunomodulation of BMMΦs and AMΦs by PMSCs impact disease outcome, we first assessed two classical MΦ antibacterial functions in both MΦ populations: bacterial phagocytosis and reactive oxygen species (ROS) production. In BMMΦs, co-culture with PMSCs surprisingly decreased in vitro bacterial phagocytosis capacity significantly (figure 6A,B), while in AMΦs, PMSC co-culture significantly increased this capacity (figure 6C,D). To assess whether PMSCs can modulate the production of antibacterial effector molecules from the two MΦ populations in vivo, we measured ROS levels in AMΦs and BMMΦs harvested from lung tissues of uninfected and KP-infected mice. ROS production by BMMΦs treated with PBS or PMSCs was similar in uninfected mice, with production rising significantly after KP infection with PBS treatment which could be partially reversed when PMSCs were administered (figure 6E,F). For AMΦs, ROS production was also similar in uninfected mice treated with PBS or PMSCs, with levels significantly increased in PBS-treated infected mice, which were further increased in PMSC-treated infected mice compared with those in uninfected groups (figure 6G,H). Moreover, we concurrently assessed phagocytosis and ROS production in both M1 and M2 BMMΦs and AMΦs, and found that PMSCs suppressed both antibacterial functions in M1 BMMΦs while boosting these functions in M2 AMΦs (online supplemental figure 4). We also excluded that PMSCs have direct antibacterial properties, finding that PMSCs does not affect *KP* growth in vitro or virulence gene expression in vivo (online supplemental figure 5). These findings collectively demonstrate that during an active bacterial infection, PMSCs modulate BMMΦs and AMΦs in divergent directions: decreasing effector antibacterial functions in BMMΦs while increasing similar functions in AMΦs.

To assess whether PMSC preferential enhancement of AMΦ antibacterial functions was critical to improving disease outcome, we depleted AMΦs but not BMMΦs prior to KP infection using intratracheal injection of clodronate (figure 6I). In uninfected mice, intratracheal clodronate did

Thorax: first published as 10.1136/thoraxjnl-2021-217928 on 21 April 2022. Downloaded from http://thorax.bmj.com/ on March 20, 2024 by guest. Protected by copyright.

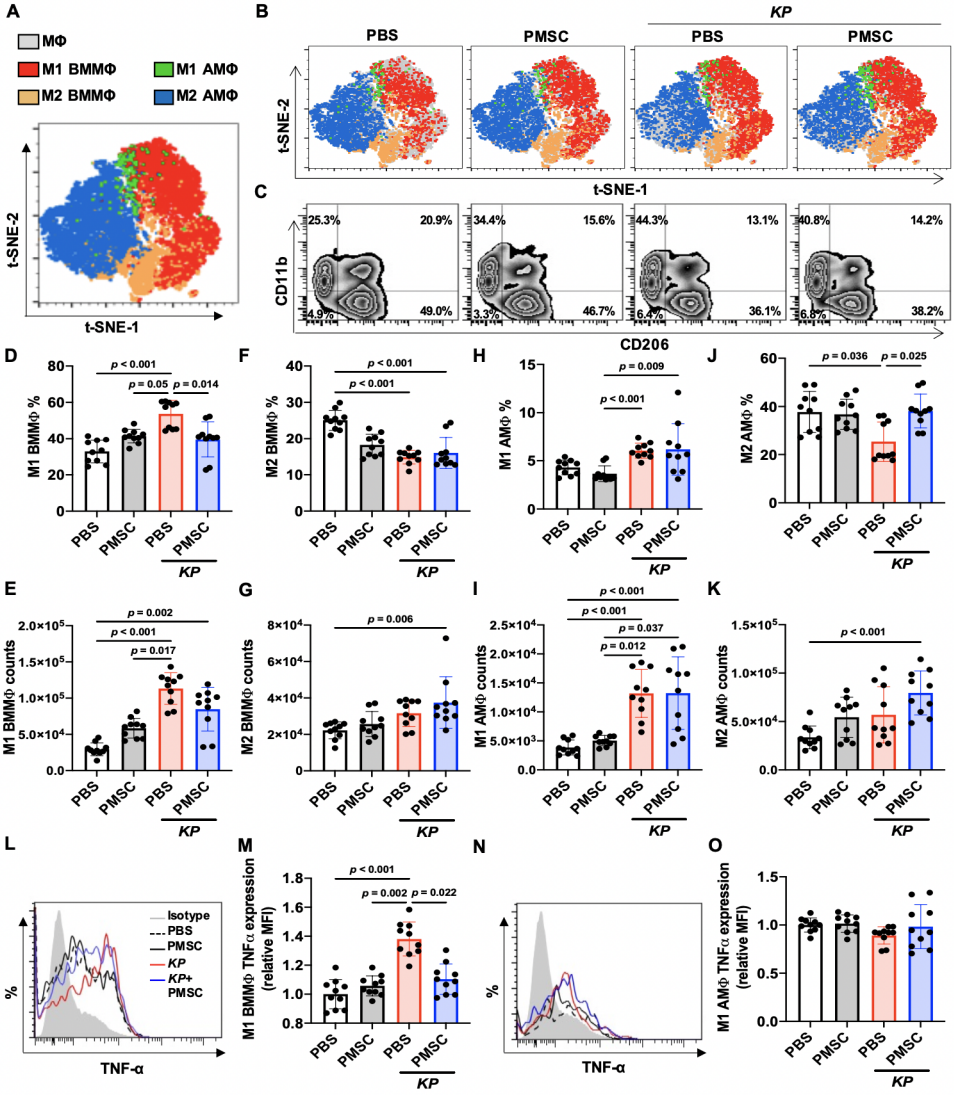

Figure 5 Human placental mesenchymal stem cells (PMSCs) reduce the population and function of M1 bone marrow MΦs (BMMΦs) while preserving M2 alveolar MΦs (AMΦ) population in mice with *Klebsiella pneumoniae* (KP) pneumonia. (A, pooled data; B, representative data) Population analyses for M1 and M2 BMMΦs as well as M1 and M2 AMΦs with PhenoGraft on the MΦ-based t-distributed stochastic neighbor embedding (t-SNE) map. Single-cell suspensions harvested from lung tissues of non-infected mice as well as infected mice injected with phosphate buffered saline (PBS) or PMSCs were stained with anti-CD45, anti-CD11b, anti-F4/80 and anti-CD206, assessed by flow cytometry and analysed with t-SNE-based algorithm. Gating for $CD45^+$ cells was first performed, and then $CD206^-CD11b^{high}F4/80^+$ M1 BMMΦs and $CD206^+CD11b^{high}F4/80^+$ M2 BMMΦs as well as $CD206^-CD11b^{low}F4/80^+$ M1 AMΦs and $CD206^+CD11b^{low}F4/80^+$ M2 AMΦs were gated on the two t-SNE dimensions. (C) Representative data for frequency analyses of M1 and M2 populations in BMMΦs or AMΦs from lung lobes as assessed with flow cytometry. Gating for $CD45^+F4/80^+$ cells was first performed, with subsequent analyses for CD11b and CD206 signals. (D, E) Pooled data for analyses of frequency and absolute number, respectively, of $CD206^-CD11b^{high}F4/80^+$ M1 BMMΦs (n=10 for each group). (F, G) Pooled data for analyses of frequency and absolute number, respectively, of $CD206^+CD11b^{high}F4/80^+$ M2 BMMΦs (n=10 for each group). (H, I) Pooled data for analyses of frequency and absolute number, respectively, of $CD206^-CD11b^{low}F4/80^+$ M1 AMΦs (n=10 for each group). (J, K) Pooled data for analyses of frequency and absolute number, respectively, of $CD206^+CD11b^{low}F4/80^+$ M2 AMΦs (n=10 for each group). (L, representative data; M, pooled data) Relative TNF-α expression levels of M1 BMMΦs as assessed in $CD45^+CD11b^{high}F4/80^+CD206^-$. Single-cell suspensions harvested from lung tissues, followed by intracellular staining of tumour necrosis factor (TNF)-α (n=10 for each group). (N, representative data; O, pooled data) Relative TNF-α expression levels of M1 AMΦs as assessed in $CD45^+CD11b^{low}F4/80^+CD206^-$ cells harvested from lung tissues, followed by intracellular staining of TNF-α (n=10 for each group). Data are shown as mean±SD.

not alter BMMΦ percentages or absolute counts (figure 6J,K), whereas AMΦ percentages and counts were sharply decreased (figure 6L,M), demonstrating a fivefold decrease specifically of AMΦs without affecting BMMΦs. Using this model, we then infected mice with LD_{50} of KP with subsequent PBS or PMSC treatment. We found that in KP-infected mice after AMΦ depletion, PMSC treatment did not significantly improve pulmonary bacterial clearance compared with PBS treatment (figure 6N). More importantly, PMSC treatment in AMΦ-depleted mice infected with sublethal KP dose not only failed to rescue mice but actually worsened the survival rate (figure 6O). These findings demonstrate that the therapeutic effects of PMSCs in severe KP pneumonia were dependent on AMΦs and their antibacterial capacities.

Thorax: first published as 10.1136/thoraxjnl-2021-217928 on 21 April 2022. Downloaded from http://thorax.bmj.com/ on March 20, 2024 by guest. Protected by copyright.

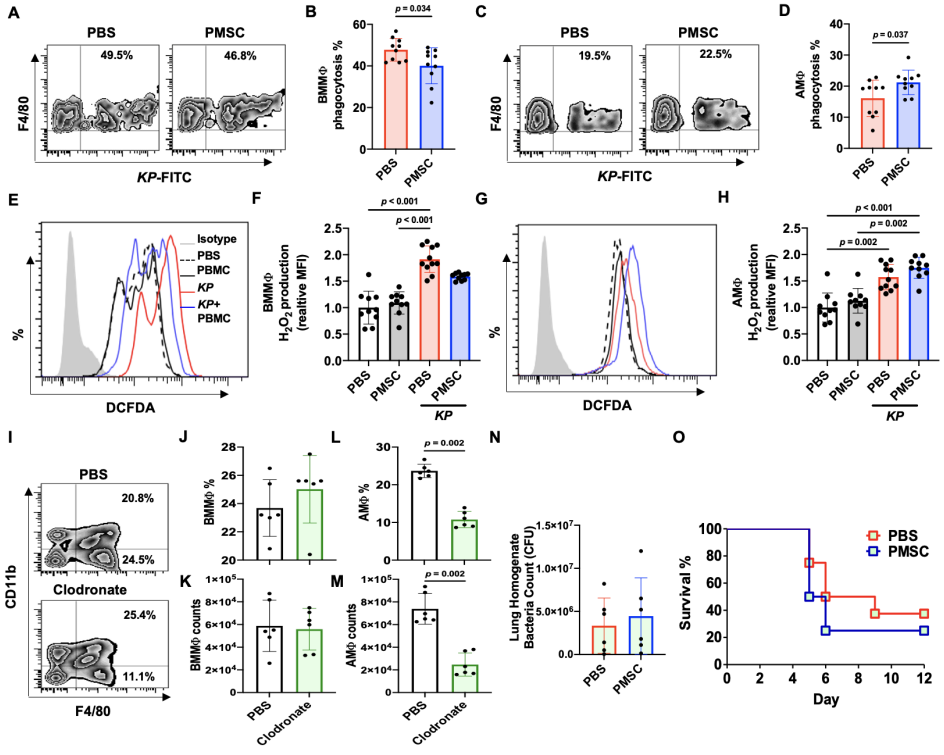

Figure 6 Human placental mesenchymal stem cells (PMSCs) enhanced multiple antibacterial functions in alveolar MΦs (AMΦs) but not bone marrow MΦs (BMMΦs) to significantly improve bacterial clearance and survival in mice with *Klebsiella pneumoniae* (KP) pneumonia which were abrogated after AMΦ depletion. (A, representative data; B, pooled data) The capability of KP phagocytosis in BMMΦs harvested from lung tissues co-cultured in phosphate buffered saline (PBS) or with PMSCs (n=10 for each group) for 2 hours as assessed with subsequent addition of FITC-labelled KP for 30 min at 37°C. Phagocytic capability of BMMΦs was measured by detecting for the frequency of $FITC^+$ cells in $CD11b^{high}F4/80^+$. (C, representative data; D, pooled data) The capability of KP phagocytosis in AMΦs harvested from lung tissues co-cultured in PBS or with PMSCs (n=10 for each group) for 2 hours as assessed with subsequent addition of FITC-labelled KP for 30 min at 37°C. Phagocytic capability of AMΦs was measured by detecting for the frequency of $FITC^+$ cells in $CD11b^{low}F4/80^+$. (E, representative data; F, pooled data) Assessment of BMMΦ respiratory burst as measured by reactive oxygen species (ROS) production of H_2O_2 in each experimental group. Isolated cells from lung tissues were incubated with 10 µM of 2′,7′-dichlorofluorescein diacetate (DCFDA) for 30 min, and then analysed by flow cytometry to assess ROS levels in $CD45^+CD11b^{high}F4/80^+$ BMMΦs (n=8 for each group). (G, representative data; H, pooled data) Assessment of AMΦ respiratory burst as measured by ROS production of H_2O_2 in each experimental group. Isolated cells from lung tissues were incubated with 10 µM DCFDA for 30 min, and then analysed by flow cytometry to assess ROS levels in $CD45^+CD11b^{low}F4/80^+$ AMΦs (n=8 for each group). (I) Representative data for frequency analyses of $CD11b^{high}F4/80^+$ BMMΦs and $CD11b^{low}F4/80^+$ AMΦs in lung lobes treated with PBS or clodronate as assessed with flow cytometry. C57BL/6J mice were intratracheally injected with 100 µL of PBS or 15 mM clodronate solution. After 2 days, single-cell suspensions harvested from lung tissues were stained with anti-CD45, anti-CD11b and anti-F4/80 for flow cytometric analyses. Gating for $CD45^+$ cells was first performed, with subsequent frequency analysis for $CD11b^{high}F4/80^+$ BMMΦs and $CD11b^{low}F4/80^+$ AMΦs. (J, K) Pooled data for analyses of frequency and absolute number of $CD11b^{high}F4/80^+$ BMMΦs, respectively (n=6 for each group). (L, M) Pooled data for analyses of frequency and absolute number of $CD11b^{low}F4/80^+$ AMΦs, respectively (n=6 for each group). (N) Assessment of bacterial load within lung homogenate in clodronate-pretreated mice infected with 5×10^6 CFU of K2 KP. Clodronate-pretreated mice were then intratracheally infected with sublethal dose (5×10^6 CFU) of K2 KP followed by intravenous administration of PBS or 3×10^5 PMSCs 2 hours later. Lung lobes were collected for detection of bacterial burden (n=6 for each group). (O) Kaplan-Meier survival analysis of clodronate-pretreated/AMΦ-depleted mice with K2 KP infection (5×10^6 CFU) after PBS or PMSC treatment. Survival was observed for 12 days (n=8 for each group). Data are shown as mean±SD.

Human PMSC-secreted IL-1β prominently increase AMΦ antibacterial functions to significantly improve KP pneumonia disease outcome

To identify which factor may be involved in the potent capacity of PMSCs to modulate and significantly increase multiple AMΦ antibacterial functions, we performed transcriptome profiling of PMSCs and MAP analysis, finding IL1B to be the most potential candidate (figure 7A).[20] To ascertain whether IL-1β is responsible for PMSC-mediated enhancement of AMΦ antibacterial functions, we assessed both in vitro KP phagocytosis and in vivo ROS production of AMΦs under KP infection with subsequent treatment of PMSCs after specific knockdown of IL1B (shIL1B-PMSCs) or non-target knockdown (shLuc-PMSCs). Compared with PBS group, co-culture with shLuc-PMSCs significantly increased AMΦ in vitro bacterial phagocytic capacity while co-culture with shIL1B-PMSCs reversed the capacity back to baseline (figure 7B–C). ROS production in AMΦs of *KP*-infected mice was significantly increased with shLuc-PMSC treatment, but not with shIL1B-PMSC treatment which resulted in levels close to PBS-treated levels (figure 7D,E). To determine whether PMSC-expressed IL-1β was critical to improving disease outcome, we first assessed bacterial clearance in KP-infected mice 4 hours post-infection. We found that the local pulmonary bacteria load in KP-infected mice after PBS treatment was significantly increased than that in infected mice treated with shLuc-PMSCs (figure 7F). However, in KP-infected mice treated with

Thorax: first published as 10.1136/thoraxjnl-2021-217928 on 21 April 2022. Downloaded from http://thorax.bmj.com/ on March 20, 2024 by guest. Protected by copyright.

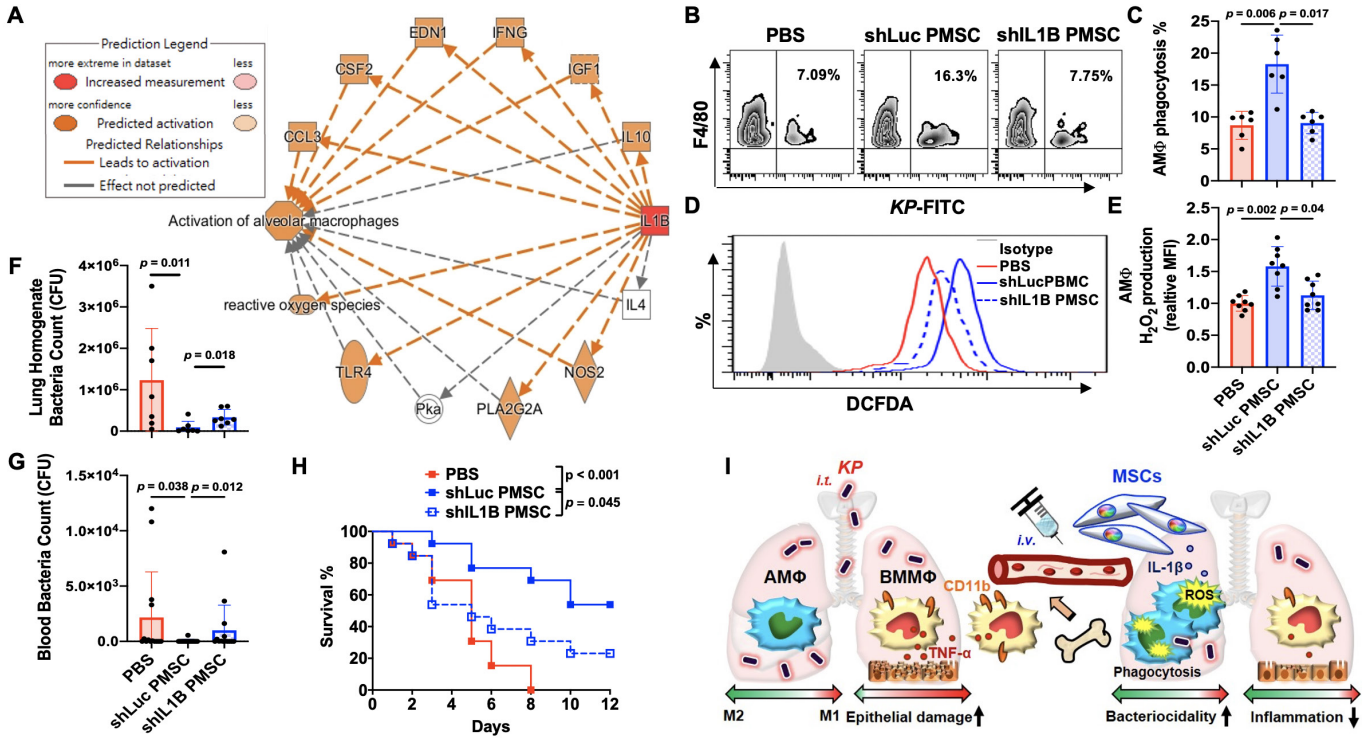

Figure 7 Human placental mesenchymal stem cell (PMSC)-secreted interleukin (IL)-1β prominently increase alveolar MΦ (AMΦ) antibacterial functions to significantly improve *Klebsiella pneumoniae* (KP) pneumonia disease outcome. (A) Pathway analysis on the process of AMΦ activation with IL1B upregulation as performed by Molecular Activation Prediction (MAP) tool in Ingenuity Pathway Analysis (IPA). The MAP tool showed that 'activation of AMΦs' is upregulated (orange) through positively regulated downstream molecules (orange lines) after upregulation of IL1B (red). (B, representative data; C, pooed data) Assessment of bacterial phagocytic capacity of AMΦs co-cultured for 2 hours with phosphate buffered saline (PBS) or PMSCs after knockdown with short hairpin RNA to luciferase (shLuc; negative control) or IL1B (shIL1B) (n=6 for each group). (D, representative data; E, pooled data) Assessment of respiratory burst in AMΦ extracted from lungs of KP-infected mice after intravenous injection of PBS, shLuc-PMSCs or shIL1B-PMSCs (n=6 for each group). (F, G) Assessment of bacterial load within lung homogenate (F; n=7 in each group) and peripheral blood (G; n=14 in each group) of KP-infected mice, respectively, of KP-infected mice after intravenous injection of PBS, shLuc-PMSCs or shIL1B-PMSCs. (H) Kaplan-Meier survival analysis of intravenous treatment of PBS, shLuc-PMSCs or shIL1B-PMSCs of mice intratracheally infected with 5×10^7 CFU of K2 KP. Survival was observed for 12 days (n=13). Data are shown as mean±SD. (F) Summary: Human PMSCs differentially enhance resident AMΦ function via IL-1β while suppressing recruited BMMΦ inflammatory function, leading to decreased local as well as systemic inflammation and significantly improving survival of mice with severe, lethal KP pneumonia.

shIL1B-PMSCs, a significantly higher bacterial load was seen when compared with levels in shLuc-PMSC-injected infected mice. The importance of PMSC-secreted IL-1β was even more prominent in reducing systemic bacterial load (figure 7G). Most importantly, treatment of shLuc-PMSCs but not shIL1B-PMSCs significantly improved survival of LD_{100}-infected mice (figure 7H). These findings demonstrate the importance of IL-1β in PMSC modulation of AMΦs to improve disease outcomes of severe bacterial pneumonia/ARDS.

DISCUSSION

The lungs are in constant contact with the environment, thus requiring resident AMΦs to maintain immune homeostasis and tissue repair,[17] and during infections, recruited BMMΦs to rapidly produce effector responses.[15] The careful orchestration in the actions of these two MΦ populations during severe bacterial infections is crucial not only for pathogen clearance but also limiting the concomitant, potentially lethal tissue injury. Thus, it is surprising that no previous reports have evaluated MSC interactions towards AMΦs and BMMΦs simultaneously, especially since MSC therapy appear particularly suited for pulmonary diseases given the tremendous first-pass effect with intravenous delivery,[27–29] effects which are further increased with inflammation.[30 31] Surprisingly, many studies of MSCs for bacterial pulmonary infections have used less clinically relevant models such as applying lipopolysaccharide (LPS) only or *Escherichia coli*, given MSCs intratracheally, or not evaluated survival.[32–35] Two reports have used more clinically relevant bacteria, such as *Streptococcus pneumoniae* but not evaluating MΦs in vivo,[36] and another used KP but treated with murine BMMSCs intratracheally[37]; neither reports studied resident AMΦs. Two other reports evaluated MSC-pulmonary MΦ interactions using *E. coli*, and found that MSCs reduced overall pulmonary MΦ inflammatory responses including enhancing bacterial phagocytosis.[38 39] However, the study did not ascertain whether the isolated pulmonary MΦs from infected lungs were truly AMΦs. MSC-CD11b^{low} AMΦ interactions have been evaluated in one early study, finding that MSC-derived medium can modulate these MΦs to an M2 phenotype after in vitro LPS stimulation.[40] Despite considerable differences in methodology and endpoints, findings collectively from these earlier studies are surprisingly similar to our more detailed investigation of MΦ subpopulations and specific roles: during pulmonary inflammation/infection, MSCs modulate MΦ populations towards an immunomodulatory M2 phenotype to decrease overexuberant inflammatory responses while enhancing antibacterial functions

Thorax: first published as 10.1136/thoraxjnl-2021-217928 on 21 April 2022. Downloaded from http://thorax.bmj.com/ on March 20, 2024 by guest. Protected by copyright.

to significantly improve tissue repair and disease outcome. Our report particularly highlights the importance of AMΦs—and PMSC treatment in supporting these MΦs quantitatively and qualitatively—in combating severe bacterial pulmonary infection and ARDS.

We demonstrate that PMSC-secreted IL-1β, the endogenous pyrogen highly produced by innate immune cells in response to infection, is critical in mediating survival benefits against severe KP pneumonia and complications. Generally considered to be immunomodulatory rather than inflammatory, PMSC production of IL-1β is unexpected, but may make sense teleologically. The placenta has few effector-phenotype immune cell populations, and it is plausible that non-immune cells such as PMSCs 'take over' these functions, although at a much less vigorous level, as the amount of IL-1β expressed by PMSCs is very low compared with levels in bacterial infection (data not shown). Further research is warranted to explore whether PMSCs have source-specific immunomodulatory properties.

Overall, we demonstrate that human PMSCs differentially modulate resident AMΦs and recruit BMMΦ in severe KP-pneumonia to minimise tissue injury and improve disease outcome, with the overall immune milieu shifted towards an M2, immunomodulatory phenotype. Specifically, PMSC-secreted IL-1β increases AMΦ antibacterial functions and is critical in improving pathogen clearance especially systemic bacteraemia, and survival (figure 7I). These findings demonstrate the distinct roles of MΦ populations in infection and recovery, as well as strongly implicate a potential therapeutic role for PMSCs in severe bacterial pneumonia/ARDS.

Author affiliations
[1]Department of Obstetrics & Gynecology, National Taiwan University Hospital & College of Medicine, Taipei, Taiwan
[2]Regenerative Medicine Research Group, Institute of Cellular & System Medicine, National Health Research Institutes, Zhunan, Taiwan
[3]Department of Obstetrics & Gynecology, Cathay General Hospital Shiji, New Taipei, Taiwan
[4]Translational Medicine Research Center, China Medical University Hospital, Taichung, Taiwan
[5]National Institute of Infectious Diseases & Vaccinology, National Health Research Institutes, Zhunan, Taiwan
[6]Division of Infectious Diseases and Tropical Medicine, Department of Internal Medicine, Tri-Service General Hospital, National Defense Medical Center, Taipei, Taiwan
[7]Division of Infection, Department of Medicine, Taipei Tzu Chi Hospital, Buddhist Tzu Chi Medical Foundation, New Taipei, Taiwan
[8]Graduate Institute of Basic Medical Science, China Medical University, Taichung, Taiwan
[9]National Institute of Cancer Research, National Health Research Institutes, Zhunan, Taiwan
[10]Institute of Clinical Pharmacy and Pharmaceutical Sciences, National Cheng Kung University, Tainan, Taiwan
[11]School of Medical Laboratory Science and Biotechnology, Taipei Medical University, Taipei, Taiwan
[12]Graduate Institute of Medicine, College of Medicine, Kaohsiung Medical University, Kaohsiung, Taiwan
[13]Graduate Institute of Microbiology & Immunology, National Defense Medical Center, Taipei, Taiwan

Correction notice This article has been corrected since it was first published. The open access licence has been updated to CC BY.

Acknowledgements We would also like to acknowledge the service provided by the Flow Cytometric Analyzing and Sorting Core Facility at the National Taiwan University Hospital, as well as technical support provided by Core Instrument Center of the National Defense Medical Center.

Contributors LTW designed the research, performed experiments, analysed the data, wrote the manuscript and provided funding; SKC and LKS provided samples, provided critical feedback and revised the manuscript; HHW, YYC, WL and LYH performed experiments; KJL and HKS analysed data; BLY and MLY conceived the idea, oversaw the research, revised the manuscript and provided funding. MLY is the guarantor for this work.

Funding This work was partially funded by the Taiwan Ministry of Science & Technology (MOST109-2326-B-002-016-MY3 to LTW, MOST107-2314-B-002-104-MY3 and MOST110-2314-B-002-042 to MLY), and the NHRI (11A1-CSPP06 & CS-111-GP-01 to BLY).

Competing interests None declared.

Patient consent for publication Not applicable.

Provenance and peer review Not commissioned; externally peer reviewed.

Data availability statement Data are available upon reasonable request.

Supplemental material This content has been supplied by the author(s). It has not been vetted by BMJ Publishing Group Limited (BMJ) and may not have been peer-reviewed. Any opinions or recommendations discussed are solely those of the author(s) and are not endorsed by BMJ. BMJ disclaims all liability and responsibility arising from any reliance placed on the content. Where the content includes any translated material, BMJ does not warrant the accuracy and reliability of the translations (including but not limited to local regulations, clinical guidelines, terminology, drug names and drug dosages), and is not responsible for any error and/or omissions arising from translation and adaptation or otherwise.

Open access This is an open access article distributed in accordance with the Creative Commons Attribution 4.0 Unported (CC BY 4.0) license, which permits others to copy, redistribute, remix, transform and build upon this work for any purpose, provided the original work is properly cited, a link to the licence is given, and indication of whether changes were made. See: https://creativecommons.org/licenses/by/4.0/.

REFERENCES

1 Fung CP, Hu BS, Chang FY, *et al*. A 5-year study of the seroepidemiology of Klebsiella pneumoniae: high prevalence of capsular serotype K1 in Taiwan and implication for vaccine efficacy. *J Infect Dis* 2000;181:2075–9.
2 Kollef MH, Shorr A, Tabak YP, *et al*. Epidemiology and outcomes of health-care-associated pneumonia: results from a large US database of culture-positive pneumonia. *Chest* 2005;128:3854–62.
3 Mulani MS, Kamble EE, Kumkar SN, *et al*. Emerging strategies to combat ESKAPE pathogens in the era of antimicrobial resistance: a review. *Front Microbiol* 2019;10:539.
4 Lin J-C, Koh TH, Lee N, *et al*. Genotypes and virulence in serotype K2 Klebsiella pneumoniae from liver abscess and non-infectious carriers in Hong Kong, Singapore and Taiwan. *Gut Pathog* 2014;6:21.
5 Deng JC, Moore TA, Newstead MW, *et al*. Cpg oligodeoxynucleotides stimulate protective innate immunity against pulmonary Klebsiella infection. *J Immunol* 2004;173:5148–55.
6 Deng JC, Zeng X, Newstead M, *et al*. Stat4 is a critical mediator of early innate immune responses against pulmonary Klebsiella infection. *J Immunol* 2004;173:4075–83.
7 Moore TA, Perry ML, Getsoian AG, *et al*. Increased mortality and dysregulated cytokine production in tumor necrosis factor receptor 1-deficient mice following systemic Klebsiella pneumoniae infection. *Infect Immun* 2003;71:4891–900.
8 Moore TA, Lau HY, Cogen AL, *et al*. Anti-Tumor necrosis factor-alpha therapy during murine Klebsiella pneumoniae bacteremia: increased mortality in the absence of liver injury. *Shock* 2003;20:309–15.
9 Torres A, Sibila O, Ferrer M, *et al*. Effect of corticosteroids on treatment failure among hospitalized patients with severe community-acquired pneumonia and high inflammatory response: a randomized clinical trial. *JAMA* 2015;313:677–86.
10 Yen BL, Huang H-I, Chien C-C, *et al*. Isolation of multipotent cells from human term placenta. *Stem Cells* 2005;23:3–9.
11 Wang L-T, Ting C-H, Yen M-L, *et al*. Human mesenchymal stem cells (MscS) for treatment towards immune- and inflammation-mediated diseases: review of current clinical trials. *J Biomed Sci* 2016;23:76.
12 Abumaree MH, Abomaray FM, Alshabibi MA, *et al*. Immunomodulatory properties of human placental mesenchymal stem/stromal cells. *Placenta* 2017;59:87–95.
13 Yen BL, Yen M-L, Wang L-T, *et al*. Current status of mesenchymal stem cell therapy for immune/inflammatory lung disorders: Gleaning insights for possible use in COVID-19. *Stem Cells Transl Med* 2020;9:1163–73.
14 Wang L-T, Liu K-J, Sytwu H-K, *et al*. Advances in mesenchymal stem cell therapy for immune and inflammatory diseases: use of cell-free products and human pluripotent stem cell-derived mesenchymal stem cells. *Stem Cells Transl Med* 2021;10:1288–303.
15 Divangahi M, King IL, Pernet E. Alveolar macrophages and type I IFN in airway homeostasis and immunity. *Trends Immunol* 2015;36:307–14.
16 Hussell T, Bell TJ. Alveolar macrophages: plasticity in a tissue-specific context. *Nat Rev Immunol* 2014;14:81–93.
17 Byrne AJ, Mathie SA, Gregory LG, *et al*. Pulmonary macrophages: key players in the innate defence of the airways. *Thorax* 2015;70:1189–96.

Thorax: first published as 10.1136/thoraxjnl-2021-217928 on 21 April 2022. Downloaded from http://thorax.bmj.com/ on March 20, 2024 by guest. Protected by copyright.

18 Moreira AP, Hogaboam CM. Macrophages in allergic asthma: fine-tuning their pro- and anti-inflammatory actions for disease resolution. *J Interferon Cytokine Res* 2011;31:485–91.
19 Wynn TA, Vannella KM. Macrophages in tissue repair, regeneration, and fibrosis. *Immunity* 2016;44:450–62.
20 Wang L-T, Wang H-H, Chiang H-C, *et al*. Human placental MSC-Secreted IL-1β enhances neutrophil bactericidal functions during hypervirulent Klebsiella infection. *Cell Rep* 2020;32:108188.
21 Lee W, Wang L-T, Yen M-L, *et al*. Resident vs nonresident multipotent mesenchymal stromal cell interactions with B lymphocytes result in disparate outcomes. *Stem Cells Transl Med* 2021;10:711–24.
22 Berg JT, Lee ST, Thepen T, *et al*. Depletion of alveolar macrophages by liposome-encapsulated dichloromethylene diphosphonate. *J Appl Physiol* 1993;74:2812–9.
23 Younes N, Zhou L, Amatullah H, *et al*. Mesenchymal stromal/stem cells modulate response to experimental sepsis-induced lung injury via regulation of miR-27a-5p in recipient mice. *Thorax* 2020;75:556–67.
24 Li X, Zhou X, Ye Y, *et al*. Lyn regulates inflammatory responses in Klebsiella pneumoniae infection via the p38/NF-κB pathway. *Eur J Immunol* 2014;44:763–73.
25 Karki R, Sharma BR, Tuladhar S, *et al*. Synergism of TNF-α and IFN-γ triggers inflammatory cell death, tissue damage, and mortality in SARS-CoV-2 infection and cytokine shock syndromes. *Cell* 2021;184:149–68.
26 Lundahl J, Halldén G, Sköld CM. Human blood monocytes, but not alveolar macrophages, reveal increased CD11b/CD18 expression and adhesion properties upon receptor-dependent activation. *Eur Respir J* 1996;9:1188–94.
27 Anjos-Afonso F, Siapati EK, Bonnet D. In vivo contribution of murine mesenchymal stem cells into multiple cell-types under minimal damage conditions. *J Cell Sci* 2004;117:5655–64.
28 Sinclair K, Yerkovich ST, Chambers DC. Mesenchymal stem cells and the lung. *Respirology* 2013;18:397–411.
29 Chambers DC, Enever D, Ilic N, *et al*. A phase 1B study of placenta-derived mesenchymal stromal cells in patients with idiopathic pulmonary fibrosis. *Respirology* 2014;19:1013–8.
30 Ortiz LA, Gambelli F, McBride C, *et al*. Mesenchymal stem cell engraftment in lung is enhanced in response to bleomycin exposure and ameliorates its fibrotic effects. *Proc Natl Acad Sci U S A* 2003;100:8407–11.
31 Parekkadan B, Milwid JM. Mesenchymal stem cells as therapeutics. *Annu Rev Biomed Eng* 2010;12:87–117.
32 Mei SHJ, McCarter SD, Deng Y, *et al*. Prevention of LPS-induced acute lung injury in mice by mesenchymal stem cells overexpressing angiopoietin 1. *PLoS Med* 2007;4:e269.
33 Hao Q, Gudapati V, Monsel A, *et al*. Mesenchymal stem cell-derived extracellular vesicles decrease lung injury in mice. *J Immunol* 2019;203:1961–72.
34 Park J, Kim S, Lim H, *et al*. Therapeutic effects of human mesenchymal stem cell microvesicles in an ex vivo perfused human lung injured with severe *E. coli* pneumonia. *Thorax* 2019;74:43–50.
35 Gupta N, Su X, Popov B, *et al*. Intrapulmonary delivery of bone marrow-derived mesenchymal stem cells improves survival and attenuates endotoxin-induced acute lung injury in mice. *J Immunol* 2007;179:1855–63.
36 Asami T, Ishii M, Namkoong H, *et al*. Anti-Inflammatory roles of mesenchymal stromal cells during acute Streptococcus pneumoniae pulmonary infection in mice. *Cytotherapy* 2018;20:302–13.
37 Hackstein H, Lippitsch A, Krug P, *et al*. Prospectively defined murine mesenchymal stem cells inhibit Klebsiella pneumoniae-induced acute lung injury and improve pneumonia survival. *Respir Res* 2015;16:123.
38 Jerkic M, Masterson C, Ormesher L, *et al*. Overexpression of IL-10 Enhances the Efficacy of Human Umbilical-Cord-Derived Mesenchymal Stromal Cells in *E. coli* Pneumosepsis. *J Clin Med* 2019;8:847.
39 Lee JW, Krasnodembskaya A, McKenna DH, *et al*. Therapeutic effects of human mesenchymal stem cells in ex vivo human lungs injured with live bacteria. *Am J Respir Crit Care Med* 2013;187:751–60.
40 Ionescu L, Byrne RN, van Haaften T, *et al*. Stem cell conditioned medium improves acute lung injury in mice: in vivo evidence for stem cell paracrine action. *Am J Physiol Lung Cell Mol Physiol* 2012;303:L967–77.

Thorax: first published as 10.1136/thoraxjnl-2021-217928 on 21 April 2022. Downloaded from http://thorax.bmj.com/ on March 20, 2024 by guest. Protected by copyright.

SUPPLEMENTAL INFORMATION

SUPPLEMENTARY METHODS

Cell culture

Human PMSCs were isolated as previously reported.[1] Term placental tissue (38–40 weeks gestation) were obtained from healthy donor mothers after obtaining informed consent approval as reviewed by the institutional review board. PMSCs were cultured in low-glucose DMEM (Invitrogen-Thermo Fisher Scientific, MA, USA), with 10% FBS (Hyclone-Thermo Fisher Scientific), 100 U/ml penicillin, 100 g/ml streptomycin and 2 mM L-glutamine (all from Gibco-Thermo Fisher Scientific).[1, 2]

Mouse model of KP-induced bacterial pneumonia and PMSC injection

A clinical *KP* strain of serotype 2 was isolated from sputum.[3] The strain was grown in 20 ml of LB broth (Alpha Biosciences, Baltimore, MD, USA) at 37°C on a shaker at 200 rpm. After overnight incubation, bacteria were then cultured in a 1:5 dilution for additional 4 hours at 37°C until an optical density of 0.9 at 600nm was reached to ascertain bacterial counts of 4×10^8 colony-forming units (CFUs)/ml. Bacteria were then diluted in sterile PBS to a sublethal dose (5×10^6 CFUs/50 µl) or lethal dose (5×10^7 CFUs/50 µl) for intratracheal (i.t.) inoculation and maintained on ice until inoculation. Bacterial pneumonia was conducted in mice according to previous report.[4] Using protocols approved by the Institutional Animal Care and Use

Committee, 6-week old C57BL/6 mice were anesthetized with intraperitoneal a Zoletil/Xylazine mixture (Zoletil: 20-40 mg/kg, Xylazine: 5-10 mg/kg, both from Sigma-Aldrich), and then inoculated intratracheally with 50 μl of the *KP* suspension. Appropriate dilutions of the inoculum were plated on LB agar plates to confirm the dose administered.[5] Control group of mice were inoculated with 50 μl of PBS. PMSCs (3 x 10^5 cells in 100μl) or PBS were intravenously injected 2 hours after *KP* injection. Mice were euthanized with CO_2 at 4 hours, with peripheral blood collected for evaluation of bacterial load and lungs collected for evaluation of bacterial load, MΦ analyses, TNF-α detection, and histological evaluation.

Enzyme-linked immunosorbent assay (ELISA)

Lung-infiltrated immune cells were harvested after mice were infected with or without K2 *KP* for 2 hours, and then cultured in the presence or absence of PMSCs *ex vivo* for 2 hours additionally, with supernatant collected for TNF-α detection by ELISA according to manufacturer's instructions (eBioscience Systems).

Histological analysis

Lung lobes were excised and then fixed with 10% formalin overnight. Fixed lung lobes were sequentially dehydrated with 20% and 30% sucrose, then subsequently embedded in optical cutting temperature compound (OCT), followed by sectioning (10 μm thick) and H&E staining. The scoring of lung tissue injury was performed by a different technician, and done

according to a previous report[6] in which interstitial damage, vasculitis, peri-bronchitis, edema, thrombus formation, and pleuritic were all evaluated—this evaluation then resulted in a score of 0 for normal/no injury, 1 = mild injury, 2 = moderate injury, 3 = severe injury, and 4 = very severe injury.

Assessment of in vivo MΦ function

Lung lobes were minced with scissors to 1mm-sized chunks and dissected with 50 U/ml DNase and 1 mg/ml type IV collagenase at 37°C for 30 minutes. An equal volume of heat inactivated FBS was added to stop the enzymatic reaction. Single-cell suspensions were harvested by filtering through 100 μm strainer, lysing red blood cells in hypotonic buffer (H_2O with 0.15 M NH_4Cl, 10 mM $KHCO_3$ and 0.1 mM Na_2-EDTA) and washing with cold PBS. Then, the single-cell suspensions derived from lung lobes were stained with APC- or APC-Cy7-anti-mouse CD45, PerCP-anti-mouse CD11b, FITC- or PE-anti-mouse F4/80, APC- or FITC-anti-mouse CD206, PE-anti-mouse inducible nitric oxide synthase (iNOS), APC-anti-mouse arginase-1 (Arg1), PE-Cy7-anti-mouse TNF-α (all from eBioscience, San Diego, CA, USA), or FITC-anti-mouse CD11c, PE-Cy7-anti-mouse SIGLEC-F, 2'-7'-dichlorofluoresceindiacetate (DCFDA, Sigma-Aldrich, MO, USA) for 30 minutes according to manufacturer's instructions, then assessed by flow cytometry or analyzed with t-Distributed Stochastic Neighbor Embedding (t-SNE)-based algorithm. CD45 was first gated for analysis of the frequency of $CD11b^{low}F4/80^{+}$ AMΦs and $CD11b^{high}F4/80^{+}$ BMMΦs, and then either iNOS and Arg1, or CD206, TNF-α,

CD11c and SIGLEC-F were analyzed for the polarization phenotypes and further confirmation of both MΦs. Reactive oxygen species (ROS) production was assessed in gated AMΦs and BMMΦs by flow cytometry.

In vivo depletion of AMΦs

C57BL/6J mice were intratracheally injected with 100 µl of PBS or 15mM clodronate (Cayman Chemical, Ann Arbor, MI, USA).[7] After 48 hours, the frequency as well as absolute numbers of $CD11b^{low}F4/80^{+}$ AMΦs and $CD11b^{high}F4/80^{+}$ BMMΦs in lung tissues were assessed by flow cytometry. The efficacy for AMΦ depletion with clodronate was similar to use of liposomal clodronate at 3 days (data not shown), in line with previous report.[7]

Bacterial phagocytosis assay

Lung lobes from non-infected mice were harvested in RPMI (Invitrogen-Thermo Fisher Scientific)-based culture medium with 10% FBS, 100 U/ml penicillin, 100 g/ml streptomycin and 2 mM L-glutamine after animal euthanasia with CO_2, washed with PBS and placed in petri dishes with 0.5 ml PBS. The lung tissues were minced with scissors to 1mm-sized chunks and dissected with 50 U/ml DNase and 1 mg/ml type IV collagenase at 37°C for 30 minutes. An equal volume of culture medium was added to stop the digestion reaction. Extracted cells were harvested by filtering with a 100 µm strainer, and red blood cells were lysed in hypotonic buffer (H_2O with 0.15 M NH_4Cl, 10 mM $KHCO_3$and 0.1 mM Na_2-EDTA, all components from Sigma-

Aldrich) and washed with cold PBS. Immune cells harvested from lung tissues were cultured with PMSCs for 2 hours, and then exposure to FITC-labeled *KP* at 37°C for 30 minutes. Suspended cells were collected and washed with cold PBS and then stained with APC-anti-mouse CD45, PerCP-anti-mouse CD11b, PE-anti-mouse F4/80. After further washing with PBS and fixing with 1% formaldehyde, CD45-gated cells were analyzed for the frequency of *KP* uptake in $CD11b^{low}F4/80^{+}$ AMΦs and $CD11b^{high}F4/80^{+}$ BMMΦs by flow cytometry.

Bacterial growth assay

KP growth was performed as we previously reported.[8] Briefly, *KP* suspensions were cultured for 2 hours and then measured by calculating colony-forming unit (CFU) in the presence or absence of PMSCs. 5 x 10^5 CFUs of live *KP* suspensions were added to culture medium or 2 x 10^4 PMSCs for 2-hour incubation, and then culture samples were serially diluted with PBS and plated on agar plates for calculation of bacterial counts.

Determination of in vivo bacterial dissemination

Lung lobes were harvested in 0.5ml cold PBS after animal euthanasia with CO_2, and then fragmented with scissors and homogenized with syringes. Aliquots from lungs and blood samples were diluted with cold PBS and plated on LB agar plates (Alpha Biosciences) at 37°C. After overnight incubation, CFUs were calculated.

Determination of in vivo expression of bacterial virulence genes

Mice were i.t. injected with a $5x10^6$ CFUs of K2 *KP* followed by i.v. administration of PBS or $3x10^5$ PMSCs 2 hours later. At 4 hours after infection, lung lobes were excised, homogenized, serial diluted with PBS, and plated on agar plates for overnight culture. Finally, single colony derived from each animal sample was picked up for PCR analyses. *KP* virulence genes including regulator of mucoid phenotype A (rmpA), activator for capsular polysaccharide synthesis (rmpA2), enterobactin synthase component B (entB) and last universal common ancestor (LUCA) as internal control were evaluated according to our previous report.[9]

RNA silencing

The lentiviral system for IL1B knockdown was obtained from the Taiwan National RNAi Core Facility (Sinica, Taipei, Taiwan). To generate lentiviruses carrying short hairpin RNA (shRNA), we co-transfected pLKO.1-shLuc (negative control; target sequence, 5'-GCGGTTGCCAAGAGGTTCCAT -3') or pLKO.1-shIL1B (target sequence, 5'-CGGCCAGGATATAACTGACTT-3') with packaging vectors, pCMVdelR8.91 and pMD.G, into 293T cells according to protocols provided by the Taiwan National RNAi Core Facility. To knockdown IL1B expression, PMSCs were infected with 10 RIU/cell of prepared lentiviruses in the presence of 8 μg/ml protamine sulfate (Sigma-Aldrich).[8] After 24 hours of infection, the viral medium was replaced with 2 μg/ml puromycin (Sigma-Aldrich)-containing culture medium and cultured for 2 days, with the surviving cells used for experimentation.

Bioinformatic analyses

Transcriptomic profiling databases were obtained from the National Center for Biotechnology Information-Gene Expression Omnibus database for bioinformatic analyses: GSE121970 generated from lung tissues of control mice or K2 *KP*-infected mice,[10] and GSE160163 generated from murine BMMΦs treated with or without TNF-α.[11] Principal component analysis (PCA) of transcriptomic profiles was performed to show the relatedness of whole transcriptomic profiles between control and *KP*-infected lung tissues using Partek® Flow® software (Partek, Inc., St. Louis, MO), while MΦ- or immune-related pathways in Gene Ontology (GO) Biological Processes were enriched by Metascape analysis; significance was set at $P < 0.01$.[12] The Molecular Activation Prediction (MAP) tool was used to interrogate networks and pathways with expression levels of involved genes by analyzing transcriptomic data of lung tissues in *KP*-infected mice versus control mice using Ingenuity Systems Pathway Analysis (IPA) software (QIAGEN, Hilden, Germany).

REFERENCES

1. Yen BL, Huang HI, Chien CC, et al. Isolation of multipotent cells from human term placenta. *Stem Cells* 2005;23:3-9.
2. Pittenger MF, Mackay AM, Beck SC, et al. Multilineage potential of adult human

mesenchymal stem cells. *Science* 1999;284:143-147.

3. Fung CP, Hu BS, Chang FY, et al. A 5-year study of the seroepidemiology of Klebsiella pneumoniae: high prevalence of capsular serotype K1 in Taiwan and implication for vaccine efficacy. *J Infect Dis* 2000;181:2075-2079.

4. Deng JC, Moore TA, Newstead MW, et al. CpG oligodeoxynucleotides stimulate protective innate immunity against pulmonary Klebsiella infection. *J Immunol* 2004;173:5148-5155.

5. Wang LT, Chiu SK, Lee W, et al. Protocol for human placental mesenchymal stem cell therapy in a murine model of intra-abdominal infection of hypervirulent Klebsiella. *STAR Protoc* 2021;2:100337.

6. Achouiti A, Vogl T, Urban CF, et al. Myeloid-related protein-14 contributes to protective immunity in gram-negative pneumonia derived sepsis. *PLoS Pathog* 2012;8:e1002987.

7. Berg JT, Lee ST, Thepen T, et al. Depletion of alveolar macrophages by liposome-encapsulated dichloromethylene diphosphonate. *J Appl Physiol (1985)* 1993;74:2812-2819.

8. Wang LT, Wang HH, Chiang HC, et al. Human Placental MSC-Secreted IL-1beta Enhances Neutrophil Bactericidal Functions during Hypervirulent Klebsiella Infection. *Cell Rep* 2020;32:108188.

9. Wang TC, Lin JC, Chang JC, et al. Virulence among different types of hypervirulent Klebsiella pneumoniae with multi-locus sequence type (MLST)-11, Serotype K1 or K2

strains. *Gut Pathog* 2021;13:40.

10. Perlee D, de Vos AF, Scicluna BP, et al. Human Adipose-Derived Mesenchymal Stem Cells Modify Lung Immunity and Improve Antibacterial Defense in Pneumosepsis Caused by Klebsiella pneumoniae. *Stem Cells Transl Med* 2019;8:785-796.

11. Karki R, Sharma BR, Tuladhar S, et al. Synergism of TNF-alpha and IFN-gamma Triggers Inflammatory Cell Death, Tissue Damage, and Mortality in SARS-CoV-2 Infection and Cytokine Shock Syndromes. *Cell* 2021;184:149-168 e117.

12. Zhou Y, Zhou B, Pache L, et al. Metascape provides a biologist-oriented resource for the analysis of systems-level datasets. *Nat Commun* 2019;10:1523.

SUPPLEMENTARY FIGURES

Figure S1

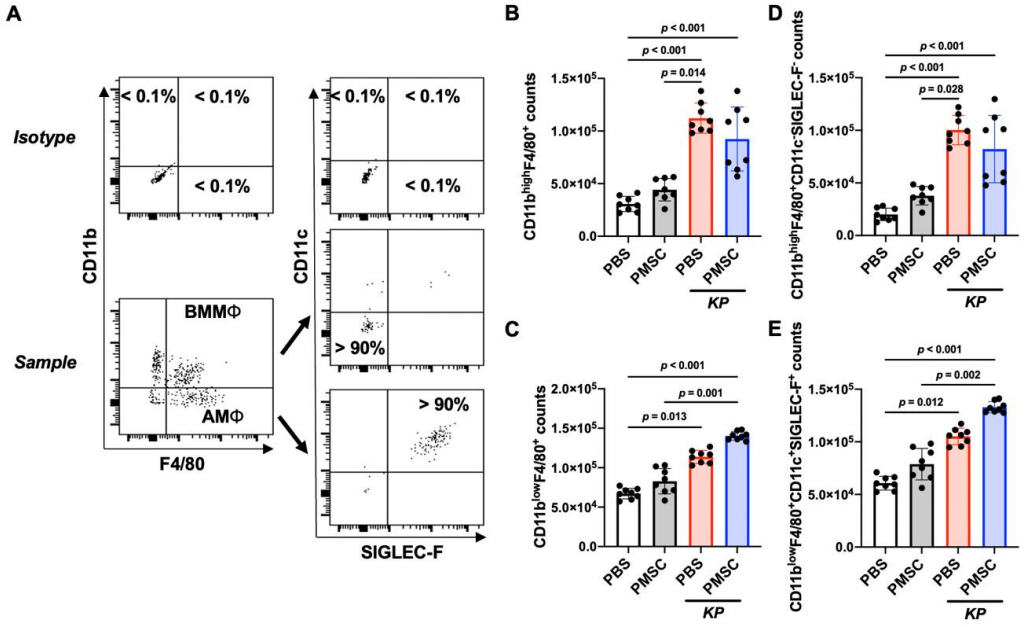

Supplementary Figure 1. Human placenta mesenchymal stem cells (PMSCs) prevent CD11b^{high}F4/80^{+} or CD11b^{high}F4/80^{+}CD11c^{-}SIGLEC-F^{-} bone marrow-derived macrophages (BMMΦs) but preserve CD11b^{low}F4/80^{+} or CD11b^{low}F4/80^{+}CD11c^{+}SIGLEC-F^{+} alveolar macrophages (AMΦs) in *KP*-infected lungs. (A) Representative data for frequency analysis of recruited BMMΦs and resident AMΦs in lung lobes as assessed with flow cytometry. C57BL/6J mice were intratracheally (i.t.) injected with 5x10^{6} CFUs of K2 *KP* followed by intravenous (i.v.) administration of PBS or 3x10^{5} PMSCs 2 hours later. Single-cell suspensions derived from lung lobes were harvested at 4 hours after infection, and then stained with anti-CD45, anti-CD11b, anti-F4/80, anti-CD11c, and anti-SIGLEC-F for flow cytometric analysis. Gating for CD45^{+} cells was first performed, with subsequent frequency analysis for

$CD11b^{high}F4/80^{+}$ BMMΦs and then the $CD11c^{-}SIGLEC\text{-}F^{-}$ population, as well as $CD11b^{low}F4/80^{+}$ AMΦs and then the $CD11c^{+}SIGLEC\text{-}F^{+}$ population. Isotype control antibodies related to all used antibodies were mixed to serve as a control for each gating protocol. (B and C) Pooled data for analyses of absolute counts of $CD11b^{high}F4/80^{+}$ BMMΦs and $CD11b^{low}F4/80^{+}$ AMΦs, respectively, in uninfected and infected lungs with or without PMSC treatment (n = 8 for each group). (D and E) Pooled data for analyses of absolute counts of $CD11b^{high}F4/80^{+}$ $CD11c^{-}SIGLEC\text{-}F^{-}$ BMMΦs and $CD11b^{low}F4/80^{+}$ $CD11c^{+}SIGLEC\text{-}F^{+}$ AMΦs, respectively, in uninfected and infected lungs with or without PMSC treatment (n = 8 for each group). Data are shown as mean ± SD.

Figure S2

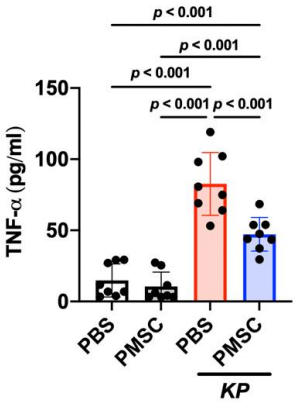

Supplementary Figure 2. Human PMSCs decrease levels of secreted TNF-α in *KP*-infected lungs. Mice were i.t. infected with $5x10^6$ CFUs of K2 *KP* followed by i.v. administration of PBS or $3x10^5$ PMSCs 2 hours later. At 4 hours after infection, mice were sacrificed and lung tissues were collected for homogenization for assessment of TNF-α by ELISA (n = 8 for each group).

Figure S3

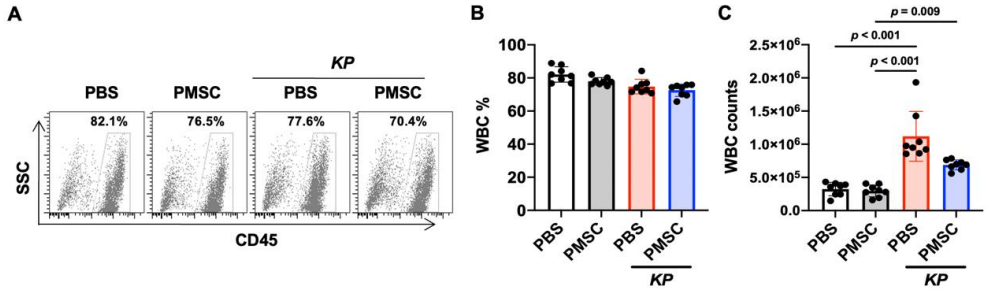

Supplementary Figure 3. Human PMSCs decrease the pulmonary infiltration of white blood cells (WBCs) in mice with pneumonia induced by clinically isolated *Klebsiella pneumonia (KP)*-serotype K2. (A & B, n=8 for each group) Representative and pooled data, respectively, of frequency of WBCs in lung lobes of each experimental group as assessed by flow cytometry. Gating for $CD45^+$ cells was performed and analyzed for frequency. (C, n=3, 3, 5, 5) Absolute number of WBCs in lung lobes of each experimental group as assessed by flow cytometry with gating for $CD45^+$ cells. Data are shown as mean ± SD.

Figure S4

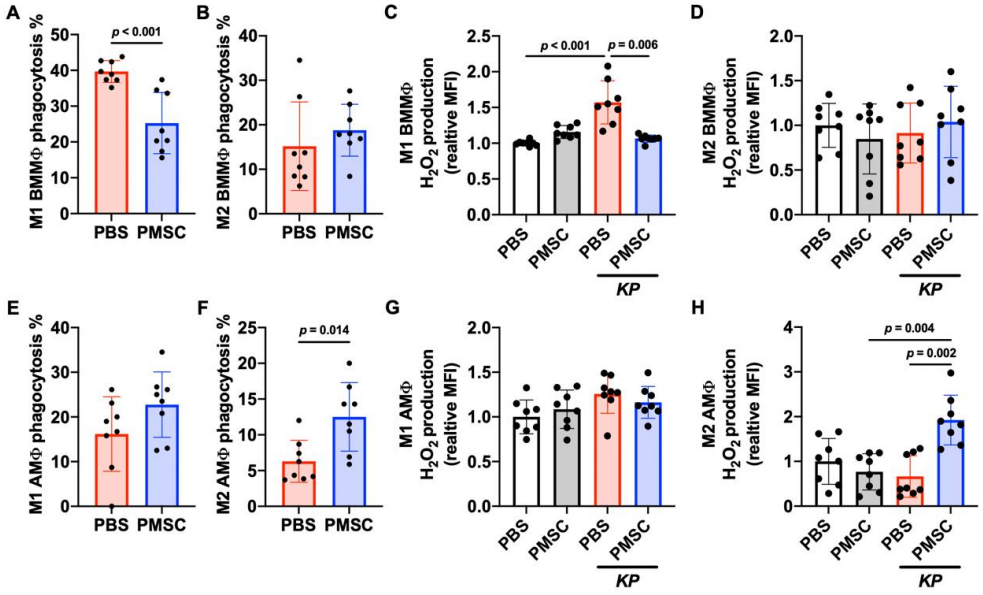

Supplementary Figure 4. Human PMSCs downregulate capabilities of phagocytosis and respiratory burst in M1-type BMMΦs while upregulating these antibacterial functions in M2-based AMΦs in mice with *KP* pneumonia. (A and B) Capabilities of *KP* phagocytosis in M1 and M2 BMMΦs harvested from lung tissues co-cultured with or without PMSCs for 2 hours as assessed with subsequent addition of FITC-labeled *KP* for 30 minutes at 37ºC. Phagocytic capabilities of M1 and M2 BMMΦs were measured by detecting for the frequency of $FITC^+$ cells in $CD45^+CD11b^{high}F4/80^+CD206^-$ and $CD45^+CD11b^{high}F4/80^+CD206^+$, respectively (n = 8 for each group). (C and D) Assessment of M1 and M2 BMMΦ respiratory burst as measured by reactive oxygen species (ROS) production of H_2O_2. Single-cell suspensions derived from lung tissues were incubated with 10 μM of 2'-7'-dichlorofluoresceindiacetate (DCFDA) for 30 minutes, and then analyzed by flow cytometry to assess ROS levels in

$CD45^+CD11b^{high}F4/80^+CD206^-$ and $CD45^+CD11b^{high}F4/80^+CD206^+$ BMMΦs (n = 8 for each group). (E and F) Capabilities of *KP* phagocytosis in M1 and M2 AMΦs derived from lung tissues co-cultured with or without PMSCs for 2 hours as assessed with subsequent addition of FITC-labeled *KP* for 30 minutes at 37ºC. Phagocytic capabilities of M1 and M2 AMΦs were measured by detecting for the frequency of $FITC^+$ cells in $CD45^+CD11b^{low}F4/80^+CD206^-$ and $CD45^+CD11b^{low}F4/80^+CD206^+$, respectively (n = 8 for each group). (G and H) Assessment of M1 and M2 AMΦ respiratory burst as measured by ROS production of H_2O_2. Single-cell suspensions derived from lung tissues were incubated with 10 μM of DCFDA for 30 minutes, and then analyzed by flow cytometry to assess ROS levels in $CD45^+CD11b^{low}F4/80^+CD206^-$ and $CD45^+CD11b^{low}F4/80^+CD206^+$ AMΦs (n = 8 for each group).

Figure S5

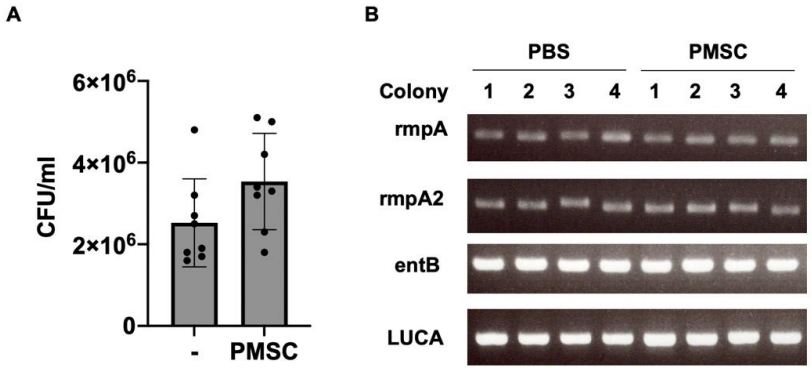

Supplementary Figure 5. Human PMSCs negligibly affect the virulence of *KP*. (A) *KP* growth as assessed by measurement of colony-forming unit (CFU) in the presence or absence of PMSCs. 5 x 10^5 CFUs of live *KP* suspension were added to culture medium or 2 x 10^4 PMSCs for 2-hour incubation, and then culture samples were serially diluted with PBS and plated on agar plates for calculation of bacterial counts. (B) PCR analyses of *KP* virulence genes including regulator of mucoid phenotype A (rmpA), activator for capsular polysaccharide synthesis (rmpA2), enterobactin synthase component B (entB), with last universal common ancestor (LUCA) as internal control. Mice were i.t. injected with a 5x10^6 CFUs of K2 *KP* followed by i.v. administration of PBS or 3x10^5 PMSCs 2 hours later. At 4 hours after infection, lung lobes were excised, homogenized, serial diluted with PBS, and plated on agar plates for overnight culture. Finally, single colony derived from each animal sample was picked up for PCR analyses.